Environ. Sci. Technol. **2001**, *35,* 1247−1251

Heterogeneous and Homogeneous Catalytic Oxidation by Supported γ-FeOOH in a Fluidized-Bed Reactor: Kinetic Approach

SHANSHAN CHOU,*,† CHIHPIN HUANG,‡ AND YAO-HUI HUANG†

Center for Environmental Safety and Health Technology, Industrial Technology Research Institute, Hsinchu, Taiwan, Republic of China, and Institute of Environmental Engineering, National Chiao Tung University, Hsinchu, Taiwan, Republic of China

Oxidation of benzoic acid (BA) by H_2O_2 was performed with a novel supported γ-FeOOH catalyst in a circulating fluidized-bed reactor (CFBR). This study focused mainly on determining the proportions of homogeneous catalysis and heterogeneous catalysis in this CFBR. Also studied herein was how pH, H_2O_2 concentration, and BA concentration affect the oxidation of BA. Experimental results indicate that the decomposition rate of H_2O_2 was proportional to its concentration and that the oxidation rate of BA depended on both H_2O_2 and BA concentrations. The change in the rate constant of heterogeneous catalysis by pH was described in terms of ionization fractions of surface hydroxyl group. From the mathematical deduction, we can infer that the reaction rate associated with $\equiv Fe^{III}OH_2^+$ is markedly higher than that with $\equiv Fe^{III}OH$. Conclusively, although heterogeneous catalysis contributes primarily to the oxidation of BA at pH 4.4−7.0, the homogeneous catalysis is of increasing importance below pH 4.4 because of the reductive dissolution of γ-FeOOH.

Introduction

Fenton's reaction, where the primary intermediate is the hydroxyl radical (•OH), is an effective and simple oxidation reaction (*1*). This reaction and its related processes have attracted increasing attention, particularly in the treatment of refractory compounds in wastewater and the remediation of contaminated soils. It has been successfully applied to degrade aromatic compounds (*2, 3*). The application of Fenton's reagent has been limited by slurry generation in which the precipitate of ferric hydroxide requires additional separation and disposal.

Iron oxide has been recently used as a catalyst for oxidizing organic contaminants with hydrogen peroxide (*4*−*7*). Al-Hayek and Dore (*4*) applied alumina-supported iron oxides in the oxidation of phenols. Goethite (α-FeOOH) particles were used to investigate heterogeneous catalytic oxidation of *n*-butyl chloride (*5*). Three iron oxides (i.e., goethite, semicrystalline, and ferrihydrite) were employed to study the decomposition kinetics of hydrogen peroxide and the degradation of quinoline (*6*). Our previous work developed a novel supported γ-FeOOH catalyst, demonstrating that it can effectively oxidize benzoic acid (BA) and 2,4,6-trichlorophenol (*7*). Our later work studied how Fe^{2+} affects the catalytic oxidation of BA by H_2O_2 and supported γ-FeOOH in the fluidized-bed reactor (*8*). Other investigations have described the catalytic decomposition of H_2O_2 by iron oxides with a modified Haber−Weiss mechanism (*4, 9*). Lin and Gurol (*10*) recently proposed a mechanism similar to the Fe^{3+}/H_2O_2 system. Both mechanisms involve an oxidation−reduction interconversion of iron oxides and a radical chain reaction.

In the batch reactor, we discovered that total iron increased with time during the oxidation of BA by H_2O_2 with this catalyst at pH 3.2 (*7*). To maintain the steady-state dissolved Fe concentration and to prevent the catalyst from the damage of mechanical mixing, we selected a fluidized-bed reactor (FBR) to conduct continuous experiments. The FBR has been extensively applied in heterogeneous catalysis due to its high efficiency in mass transfer. Although FBR has been used in some treatment processes of environmental engineering, such as anaerobic biological treatment of wastewater, incineration of wastes and volatile organic compounds, and softening of drinking water by crystallization, the potential of applying FBR in advanced oxidation processes is still unknown and deserves an in-depth investigation for commercial application.

This study evaluates the performance of the circulating FBR (CFBR) with the supported γ-FeOOH catalyst. This CFBR with a high recycle ratio is modified from normal FBR without recycle. When the recycle ratio is sufficiently large, the performance of CFBR resembles that of a continuous stirred tank reactor (CSTR) (*11, 12*). BA was selected as the target organic compound because of its nonvolatility and being the intermediate of many aromatic compounds. Although it is not a biorefractory chemical, it reacts with •OH similarly as other aromatic compounds do (*13*). Our previous study indicated that the oxidation of BA in this heterogeneous system under acidic conditions can induce homogeneous catalytic oxidation (*7*). Therefore, this study also focuses on determining the proportion of homogeneous and heterogeneous catalysis. The effects of pH, H_2O_2 concentration, and BA concentration on the oxidation of BA by our novel catalyst are also included.

Experimental Section

Catalyst Preparation and Characterization. A novel catalyst, iron oxide on a brick grain support, was developed in the following manner (*14*). The brick grains were packed in a 6.1-L (6.8 cm ϕ × 170 cm height) CFBR as carriers. H_2O_2 (Union Chemical) and $FeSO_4$ (Merck) were fed continuously with a molar ratio of 1:2 into the reactor bottom. On the surface of brick grains, the crystals were grown for 1 week before the application. The pH of the solution was controlled at 3.5 to prevent $Fe(OH)_3$ precipitation. The properties of the catalyst prepared from the CFBR have been listed in our previous work (*12*). The number of fluoride-binding surface sites (mol/g) was determined following the method of Sigg and Stumm (*15*). Intrinsic acidity constants (K_{a1} and K_{a2}) were obtained from graphic extrapolation of transformed acid−base titration data to zero surface charge conditions according to the procedure outlined by Stumm (*16*). The major component coated on the catalyst surface was identified as γ-FeOOH with a Mössbauer spectrometer (Austin S-600).

Analytical Methods. Benzoic acid and H_2O_2 were analyzed using HPLC with a reverse-phase Merck LiChrospher C-18

* Corresponding author fax: 886-3-5732349; e-mail: 790512@itri.org.tw.

† Industrial Technology Research Institute.

‡ National Chiao Tung University.

10.1021/es001129b CCC: $20.00
Published on Web 02/10/2001

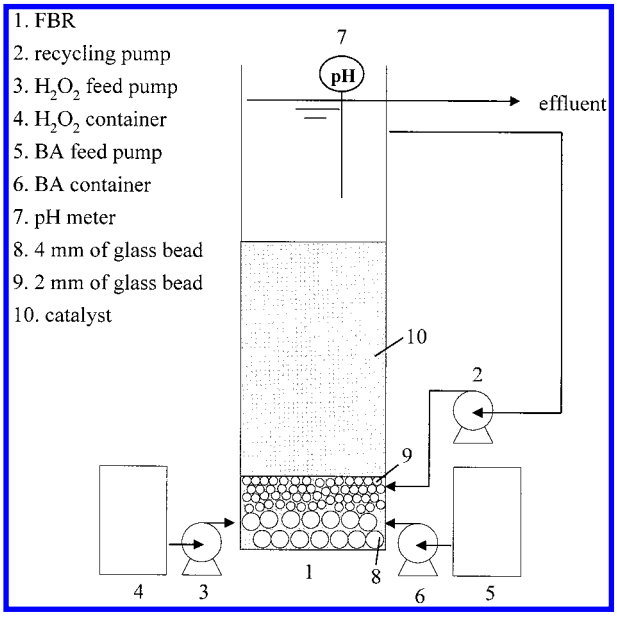

FIGURE 1. Schematic diagram of the fluidized-bed reactor.

column (25 cm length × 4 mm i.d.); the mobile phase contained 40% methanol (Fisher) and 60% deionized water with tetra-*n*-butylammonium phosphate PICA reagent (paired ion chromatography reagent for acid, TCI). Total iron concentration was determined by an atomic absorbance spectrophotometer (Varian Spectra AA-30).

Catalytic Oxidation. All of experiments were conducted at room temperature (24 ± 4 °C). The schematic apparatus is shown as Figure 1. Two bench-scale CFBRs were packed with 4 and 2 mm of glass beads on the bottom separately and then the desired amount of supported γ-FeOOH catalyst grains. The smaller one (2 cm ϕ × 100 cm height) was used to study the kinetics of heterogeneous catalytic oxidation alone and the long-term stability of γ-FeOOH catalytic performance; the larger one (3 cm ϕ × 200 cm height) was applied to determine the proportions of homogeneous and heterogeneous catalytic oxidation. The total volumes (i.e., the volume of reactor and recycling line) of these two reaction system are 600 and 1000 mL, respectively. In the smaller CFBR, the bed heights of the fixed form and the expanded form are respectively 32 and 50 cm, while in the larger CFBR, these two bed heights are 83 and 120 cm. The recycle ratio of CFBR was kept between 10 and 30. By controlling the inlet flow and internal circulation, the superficial velocity could be maintained at 40−60 m/h. Both BA and H_2O_2 were introduced with equal flow rate. The inlet concentration of BA ranged from 1.44 to 1.86 mM. The applied flow rate and H_2O_2 concentration were determined from the desired residence time (τ) and H_2O_2 dosage, respectively. To maintain a stable pH during the reaction, pH was regulated by adding acid into the H_2O_2 feed container before the experiment instead of adding acid into the reactor during the experiment. The effluent was collected by two vials at three different time after 5 times the residence time (i.e., 5τ, 6τ, and 7τ) to ensure that the reaction was at steady state (*17*). The sample in one vial was filtered for the analyses of H_2O_2 and BA; the other was mixed with concentrated H_2SO_4 to pH < 1 to determine total iron concentration (C_{Fe}, including soluble iron and iron in the fine particles). The average experimental values of three different samples were used for the data analysis. Benzoic acid can be oxidized to byproducts (such as oxalic acid) and then completely to CO_2 using our γ-FeOOH catalyst (*7*); however, we only discuss the disappearance of BA rather than the mineralization of BA in this study.

Batch Adsorption. The batch adsorption experiment was performed by transferring 3 g of supported γ-FeOOH in a 300-mL 0.01 M $NaClO_4$ solution. The pH was adjusted with $HClO_4$ and NaOH, and the solution was shaken with a reciprocating shaker at 25 °C. After the first 1 h, a given amount of BA was added, and the pH was readjusted. After 24 h of the adsorption, the suspension pH was measured, and the filtered sample was analyzed for BA.

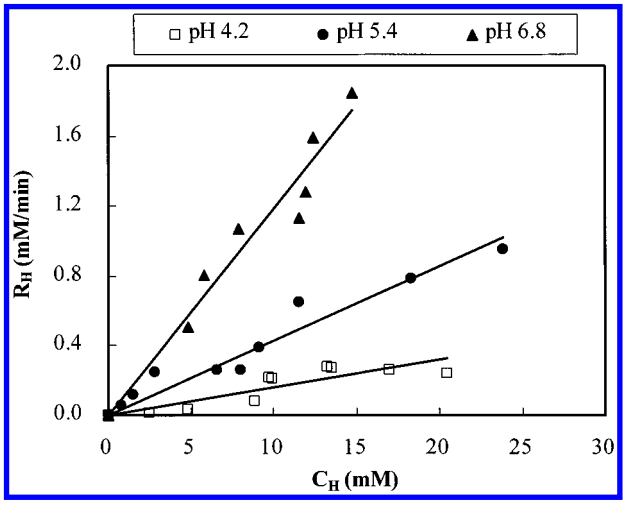

FIGURE 2. Effect of H_2O_2 concentration on decomposition of H_2O_2 in the presence of BA. C_{BAi} = 1.44−1.67 mM, τ = 36.6 min, m = 167 g/L; m denotes the catalyst concentration.

Results and Discussion

To simplify the kinetic equation, this work assumed that the CFBR used in this study can be regarded as a CSTR (*11*, *12*). According to the mass balance of H_2O_2 and BA in the CSTR, the decomposition rate of H_2O_2 (R_H) and the oxidation rate of BA (R_{BA}) can be determined directly from the inlet and outlet concentrations:

$$R_H = \frac{C_{Hi} - C_H}{\tau} \quad (1)$$

$$R_{BA} = \frac{C_{BAi} - C_{BA}}{\tau} \quad (2)$$

where C_{Hi} and C_H denote the respective inlet and outlet H_2O_2 concentrations at steady state, and C_{BAi} and C_{BA} denote the inlet and outlet BA concentrations, respectively.

Heterogeneous Catalytic Oxidation Alone. The effects of H_2O_2 concentration on the decomposition of H_2O_2 and oxidation of BA were investigated first. According to Figure 2, R_H is proportional to C_H in the experiments under three pH values (i.e., 4.2, 5.4, and 6.8). Our previous study (*12*) proved that R_H is proportional to both H_2O_2 and catalyst concentrations in the absence of BA, which conforms to the results of other investigations (*5*, *6*). We assume that the homogeneous catalysis is insignificant because all the outlet total iron concentrations are very low (i.e., <1.5 mg/L), so heterogeneous catalysis plays a major role in the above reactions. According to those investigations, the iron content of the catalyst surface is the key factor in catalyzing the decomposition of H_2O_2. Because the iron content is proportional to the catalyst concentration, we define the observed second-order rate constant in decomposing H_2O_2 (k_{obs}) based on a simplified kinetic relationship (*12*):

$$k_{obs} = \frac{R_H}{C_H S_T} \quad (3)$$

TABLE 1. Calculated and Predicted k_{obs} Values at pH 4.2, 5.4, and 6.8

pH	calcd k_{obs} (min^{-1} M^{-1})	pred k_{obs}[a] (min^{-1} M^{-1})
4.2	0.161	0.185 ± 0.185
5.4	0.435	0.331 ± 0.299
6.8	1.21	1.43 ± 0.33

[a] Expressed as 95% confidence interval, which is obtained in the absence of BA.

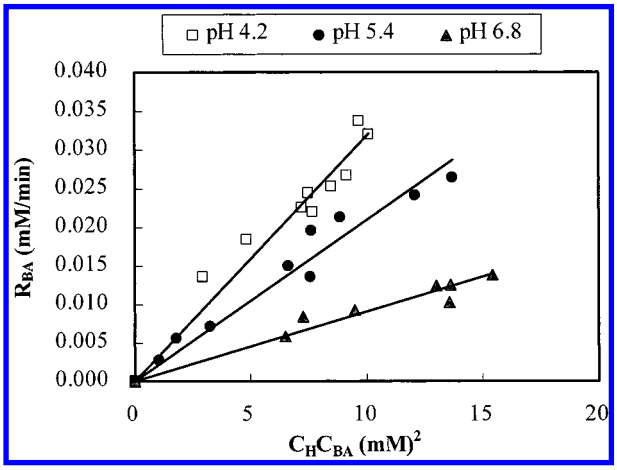

FIGURE 3. Relationship between R_{BA} and C_HC_{BA} in oxidation of BA by H_2O_2. The experimental conditions are the same as in Figure 2.

where S_T denotes the total concentration of active surface sites (i.e., 5.89×10^{-4} mol/g × catalyst concentration (g/L), as indicated in ref *12*).

According to eq 3, the k_{obs} values at pH 4.2, 5.4, and 6.8 can be calculated, as listed in Table 1. In our previous study (*12*), we have predicted k_{obs} values in the absence of BA with a fitted model. Those predicted k_{obs} values with 95% confidence intervals are also shown in Table 1. Because the experimental k_{obs} values in the presence of BA fall within the confidence intervals of predicted k_{obs} values in the absence of BA, it is possible that the decomposition of H_2O_2 is independent of the presence of BA at pH 4.2−6.8.

The kinetic model from Lin (*5*) simplifies for low organic and H_2O_2 concentrations to describe the oxidation of *n*-butyl chloride by H_2O_2 and goethite in the batch reactor as follows:

$$(R_M)_s = K[M][H_2O_2][FeOOH] \quad (4)$$

where $(R_M)_s$ is the oxidation rate of the organic compound; K is the overall reaction constant; [M], [H_2O_2], and [FeOOH] denote the concentrations of the organic compound, H_2O_2, and goethite in the solution, respectively. Figure 3 shows a test of eq 4 for our results in the oxidation of BA by H_2O_2 and supported γ-FeOOH catalyst. A linear relationship between R_{BA} and C_HC_{BA} is obtained in this figure; therefore, R_{BA} can be written as

$$R_{BA} = k_{BA}C_HC_{BA} \quad (5)$$

where k_{BA} is the observed rate constant for oxidizing BA. This equation resembles eq 4 based on a constant heterogeneous catalyst concentration. In Figure 3, the k_{BA} values, the slopes of the curves, decrease with an increasing pH. This occurrence may be attributed to the stronger binding between H_2O_2 and FeOOH at higher pH (*12*), resulting in reduced surface sites occupied by BA.

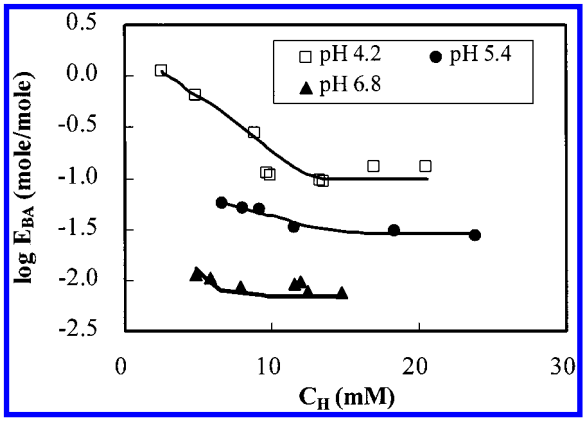

FIGURE 4. Relationship between E_{BA} and C_H in oxidation of BA by H_2O_2. The experimental conditions are the same as in Figure 2.

The performance of catalyst can be evaluated by stoichiometric efficiency (E_{BA}) as below (*6*, *18*):

$$E_{BA}\,(\text{mol/mol}) = (C_{BAi} - C_{BA})/(C_{Hi} - C_H) \quad (6)$$

In the batch reactor, it was found that this catalyst has higher E_{BA} than goethite at pH 4.3 (*7*). Using the experimental data at pH 4.2, 5.4, and 6.8, E_{BA} under three pH conditions can be calculated. In Figure 4, the relationships between E_{BA} and C_H under three pH conditions are depicted. It shows that the E_{BA} of all three pH values decreases with increasing C_H and remains unchanged after reaching the lowest values, which indicates that the radicals undergo inefficient scavenging reaction at higher C_H (*19*). This phenomenon may be interpreted by the following reaction:

$$H_2O_2 + {}^{\bullet}OH \rightarrow HO_2^{\bullet} + H_2O \quad (7)$$

where $HO_2^{\bullet}$ is the perhydroxyl radical, which is a relatively weak oxidant as compared to $^{\bullet}OH$. The E_{BA} values at pH 4.2 (i.e., 0.09−1.1) are shown to be markedly higher than those at pH 5.4 and pH 6.8 (i.e., 0.007−0.06), which is similar to the result of Khan and Watts (*20*). The decrease in E_{BA} at higher pH is influenced by an increase in k_{obs}, i.e., more rapid H_2O_2 decomposition. Miller and Valentine (*19*) proposed a reaction scheme for iron oxide surface catalyzed oxidation of quinoline by H_2O_2. This reaction scheme explains that the decrease in E_{BA} at a higher pH is attributed to an increase of radical scavenging.

Homogeneous and Heterogeneous Catalytic Oxidation. The experiments were performed in the large reactor (3 cm $\phi \times$ 200 cm height) under various pH conditions to investigate the pH effect on the BA oxidation. Table 2 lists k_{BA}, and total Fe (C_{Fe}) of the CFBR effluent where k_{BA} values were calculated from eqs 2 and 5. It can be seen that C_{Fe} was below 0.07 mM within pH 4.4−7.0 but increased dramatically at pH < 4.0. This finding suggests that homogeneous catalysis may play an important role in the acidic condition. It is important to discuss if iron is generated as Fe^{2+} by reductive dissolution of FeOOH (eq 8) (*21*, *22*) or Fe^{3+} by simple dissolution (eq 9) (*22*). Our control experiment (0.75 mM Fe^{3+}, pH 3.1, without FeOOH) shows that the catalytic performance of Fe^{3+} is very poor (data not shown). McBride (*23*) detected trace levels of Fe^{2+} during the oxidation of phenolic compounds by goethite, so he suggested that Fe^{2+} was generated via electron transfer and then was oxidized to Fe^{3+}. Lu et al. (*24*) also proved that the dissolved iron was initially formed as Fe^{2+} in the oxidation of 2-chlorophenol by goethite. Therefore, we consider that

TABLE 2. Various k_{BA} Values, C_{Fe}, and Proportions of Heterogeneous and Homogeneous Catalysis under Different pH Values for Oxidizing BA[a]

pH	k_{BA}[b] (min^{-1} mM^{-1})	C_{Fe} (mM)	P_{hete}[c] (%)	P_{homo}[d] (%)	k_{hete}[e] (min^{-1} mM^{-2})	k_{homo}[f] (min^{-1} mM^{-2})
3.1	0.139	0.755	14.4	85.6	5.76×10^{-5}	0.158
3.4	0.133	0.670	15.0	85.0	5.73×10^{-5}	0.169
3.6	0.114	0.568	17.3	82.7	5.70×10^{-5}	0.166
4.0	0.0305	0.371	63.5	36.5	5.58×10^{-5}	0.030
4.4	0.0174	0.068	~100	~0	5.00×10^{-5}	~0
4.7	0.0157	0.036	~100	~0	4.52×10^{-5}	~0
5.3	0.0165	0.027	~100	~0	4.75×10^{-5}	~0
6.0	0.0080	0.018	~100	~0	2.31×10^{-5}	~0
6.7	0.0043	0.007	~100	~0	1.25×10^{-5}	~0
7.0	0.0042	0.024	~100	~0	1.22×10^{-5}	~0

[a] C_{Hi} = 11.1−12.2 mM, C_{BAi} = 1.55−1.86 mM, τ = 50 min, m = 590 g/L. [b] Calculated from eq 5. [c] P_{hete} (proportion of heterogeneous catalysis) = $(k_{hete}S_T)/k_{BA} \times 100\%$. [d] P_{homo} (proportion of homogeneous catalysis) = (1 - P_{hete}) × 100%. [e] Calculated from eq 19. [f] Calculated from eq 20.

the increase of C_{Fe} with the decreasing pH is due to the reductive dissolution of FeOOH.

$$FeOOH_{(s)} + 3H^+ + e^- \rightarrow Fe^{2+} + 2H_2O \quad (8)$$

$$FeOOH_{(s)} + 3H^+ \rightarrow Fe^{3+} + 2H_2O \quad (9)$$

To distinguish the contribution of heterogeneous and homogeneous catalysis to BA oxidation at steady state, we consider the following two reactions in parallel:

$$BA + H_2O_2 + \gamma\text{-FeOOH} \xrightarrow{k_{hete}} \text{oxidation products} \quad (10)$$

$$BA + H_2O_2 + Fe^{2+} \xrightarrow{k_{homo}} \text{oxidation products} \quad (11)$$

where k_{hete} and k_{homo} are the rate constants of heterogeneous and homogeneous catalysis, respectively. Therefore, eq 5 can be transformed to eq 12 by replacing k_{BA} with $(k_{hete}S_T + k_{homo}C_{Fe})$:

$$R_{BA} = (k_{hete}S_T + k_{homo}C_{Fe})C_H C_{BA} \quad (12)$$

To clarify the presence of homogeneous catalysis within the pH range of 4.4−7.0, this work also performed another control experiment by introducing 0.07 mM Fe^{2+} instead of γ-FeOOH in the CFBR. Since no degradation of BA was found, we suggested that such low concentration of dissolved iron has no catalytic capability to oxidize BA in the control experiment. Hence, within pH 4.4−7.0, it is reasonable to simplify eq 12 by considering only the heterogeneous catalysis:

$$k_{BA} = k_{hete}S_T \quad 4.4 \le pH \le 7.0 \quad (13)$$

Using the data of k_{BA} in this pH range allows us to model the function for heterogeneous catalysis. As generally assumed, the active surface site consists of four surface species $\equiv Fe^{III}OH_2^+$, $\equiv Fe^{III}OH$, $\equiv Fe^{III}O^-$, and $\equiv Fe^{III}L$, where $\equiv Fe^{III}L$ denotes the surface complex of ligand (i.e., BA). The concentration profiles of these species can be calculated based on pH dependence of BA adsorption and equilibrium relations between the surface complexation species. The pH edge of BA adsorption is shown in Figure 5. It indicates that the adsorption of BA decreased with an increasing pH and no significant adsorption was observed beyond pH_{pzc} (point of zero charge) of this catalyst (i.e., pH 7.05, as indicated in ref *12*). The equilibrium expressions for surface complexation reaction can be obtained from Stumm (*16*), as listed in Table 3. $[\equiv Fe^{III}OH_2^+]$ and $[\equiv Fe^{III}O^-]$ can be expressed in terms of $[\equiv Fe^{III}OH]$ without correction for electrostatic interaction, as shown in eqs 14 and 15. $[\equiv Fe^{III}L]$ was estimated with the experimental data of BA adsorption.

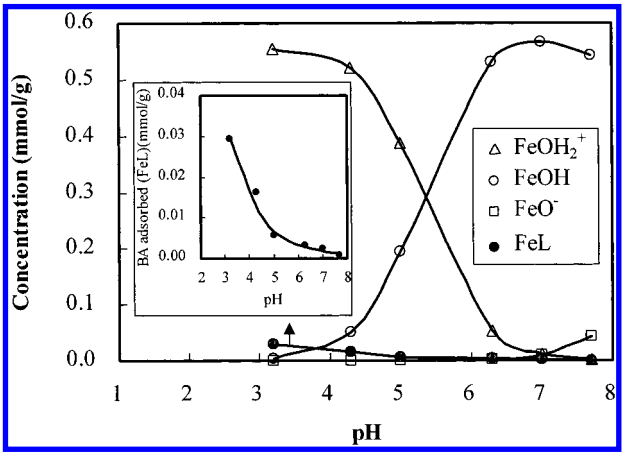

FIGURE 5. Concentration profiles of surface species $Fe^{III}OH_2^+$, Fe^{III}-OH, $Fe^{III}O^-$, and $Fe^{III}L$ in surface complexation. C_{BAi} = 0.95 mM, m = 10 g/L.

TABLE 3. Equilibrium Expressions and Mass Balance Equations for Surface Complexation Reaction[a]

$\equiv FeOH_2^+ = \equiv FeOH + H^+$	$\log K_{a1} = -5.3$
$\equiv FeOH = \equiv FeO^- + H^+$	$\log K_{a2} = -8.8$
$\equiv FeOH + HL = \equiv FeL + H_2O$	$\log K_L$
$HL = H^+ + L^-$	$\log K_{HL} = -4.2$
$S_T = [\equiv FeOH_2^+] + [\equiv FeOH] + [\equiv FeO^-] + [\equiv FeL]$	
$BA_T = [HL] + [L^-] + [\equiv FeL]$	

[a] HL, benzoic acid; L^-, benzoate, i.e., $C_{BA} = HL + L^-$.

$$[\equiv Fe^{III}OH_2^+] = [\equiv Fe^{III}OH][H^+]/K_{a1} \quad (14)$$

$$[\equiv Fe^{III}O^-] = [\equiv Fe^{III}OH]K_{a2}/[H^+] \quad (15)$$

The mass balance for total surface sites of γ-FeOOH and total amount of BA can be expressed as

$$S_T = [\equiv Fe^{III}OH]\left(\frac{[H^+]}{K_{a1}} + 1 + \frac{K_{a2}}{[H^+]}\right) + [\equiv Fe^{III}L] \quad (16)$$

$$BA_T = [HL]\left(1 + \frac{K_{HL}}{[H^+]}\right) + [\equiv Fe^{III}L] \quad (17)$$

where BA_T denotes the total amount of BA. In Figure 5, the concentration profiles of these four surface species in surface complexation under different pH values are depicted. Note that $[\equiv Fe^{III}O^-]$ and $[\equiv Fe^{III}L]$ are relatively low within pH 4.4−7.0. As generally assumed, each species has a different reaction rate with respect to the oxidation of BA, which is similar to the approach proposed by Butler and Hayes (*25*). Equation 12 can therefore be written as eq 18 by neglecting the contribution of $\equiv Fe^{III}O^-$ and $\equiv Fe^{III}L$ in this pH range:

$$(k_{hete}S_T)C_H C_{BA} = (k_{hete}^+[\equiv Fe^{III}OH_2^+] + k_{hete}^0[\equiv Fe^{III}OH])C_H C_{BA} \quad (18)$$

where k_{hete}^+ and k_{hete}^0 represent the rate constants associated with $\equiv Fe^{III}OH_2^+$ and $\equiv Fe^{III}OH$, respectively. The relationship can be further simplified to

$$k_{hete} = k_{hete}^+\alpha^+ + k_{hete}^0\alpha^0 \quad (19)$$

where $\alpha^+ = [\equiv Fe^{III}OH_2^+]/S_T$ and $\alpha^0 = [\equiv Fe^{III}OH]/S_T$.

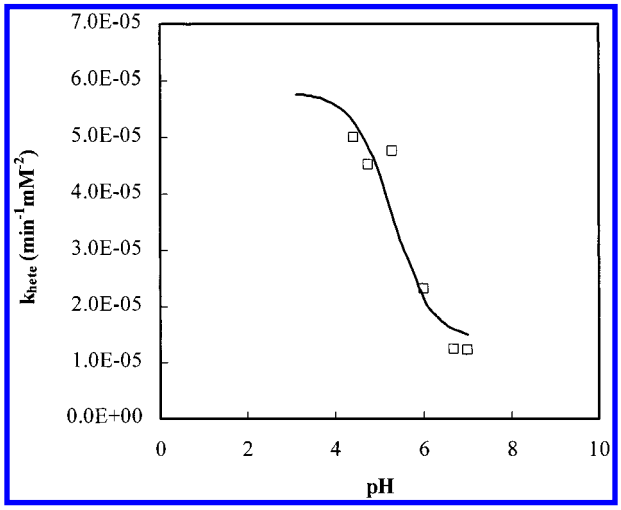

FIGURE 6. Model fitting of k_{hete} by H_2O_2 at different pH values. C_{Hi} = 11.1−12.2 mM, C_{BAi} = 1.56−1.86 mM, τ = 50 min, m = 590 g/L.

The k_{hete} values can be estimated from eq 13 and then be fitted with eq 19 using multiple regression of statistical technique. Two rate constants were determined as $k_{hete}^{+} = 5.79 \times 10^{-5}$ min^{-1} mM^{-2} and $k_{hete}^{0} = 1.43 \times 10^{-5}$ min^{-1} mM^{-2} ($r^2 = 0.891$). It shows that the reaction rate associated with $\equiv Fe^{III}OH_2^{+}$ is markedly higher than that with $\equiv Fe^{III}OH$. Electrostatic attraction may be the major force to cause such a high reaction rate for BA oxidation on the sites of $\equiv Fe^{III}$-OH_2^{+}. To test the significance of regression, we calculate the statistic F from the analysis of variance. Since F (= 16.4) > $F_{0.05,(2,3)}$ (= 9.6), we conclude that α^{+} and α^{0} contribute significantly in predicting k_{hete}. The experimental result fitted with model parameters is shown in Figure 6; therefore, a k_{hete} value of 5.7×10^{-5} min^{-1} mM^{-2} at pH 3.1−4.0 can be obtained from this figure.

Furthermore, k_{homo} can be determined by transforming eq 12 into eq 20:

$$k_{homo} = (k_{BA} - k_{hete}S_T)/C_{Fe} \qquad (20)$$

The calculated k_{homo} values at various conditions are also listed in Table 2. At pH 3.1−3.6, the k_{homo} values are nearly constant (i.e., 0.158−0.169 min^{-1} mM^{-2}) and the k_{homo} value at pH 4.0 decreases to 0.03 min^{-1} mM^{-2}. Kuo (*18*) also found that the best pH value for treatment of dye wastewater with Fenton's reaction is below 3.5.

Accordingly, the proportion of heterogeneous and homogeneous catalysis for oxidizing BA can be estimated, as shown in Table 2. This table indicates that the oxidation of BA at pH 4.4−7.0 is contributed by the heterogeneous catalysis alone. Below pH 4.4, however, the homogeneous catalysis plays an increasingly important role.

Long-Term Stability of γ-FeOOH Catalytic Performance. To discuss the kinetics of heterogeneous catalysis, we focus on experimental results of the pH range 4.4−7.0 in the preceding two sections because of little Fe dissolution in the CFBR effluent. However, Table 2 and Figure 4 show that BA degradation rate and the stoichiometric efficiency are both increasing with decreasing pH. To assess the potential for commercial application of γ-FeOOH catalyst, a 3-month long-term operation of CFBR was performed to treat three different real dyeing−finishing wastewaters within pH 3.5−4.0. The experimental results are shown in Table 4. This table proves good performance of this catalyst during the long-term operation. Furthermore, the operation with Fe^{2+} addition (as named FBR−Fenton method) can improve the catalytic performance (*8*). After this long-term operation, three trials of BA oxidation as mentioned in Table 2 (i.e., pH 3.4, 4.0, and 4.7) were repeated to test the stability of the catalyst. The results (not shown) indicate that BA concentrations of CFBR effluent and k_{BA} values in the repeated runs are 90−102% of those in the preceding section. Therefore, we conclude that the catalytic performance of γ-FeOOH is nearly unaffected by the above long-term operation for the treatment of real wastewater.

TABLE 4. Long-Term Operation of CFBR in Treating Real Dyeing−Finishing Wastewater[a]

wastewater type	C_{Fei}[b] (mM)	COD_i[c] (mg/L)	COD_e[d] (mg/L)
A	0	198	118−130
A	0.9	185−210	85−97
B	0	200	128−142
B	0.9	188−205	95−105
C	0.9	195	88−100

[a] C_{Hi} = 5.7−6.0 mM, τ = 52 min, m = 133 g/L, pH = 3.5−4.0. [b] Inlet Fe^{2+} concentration of CFBR. [c] Inlet COD concentration of CFBR. [d] COD concentration of CFBR effluent.

Acknowledgments

The authors thank Dr. S. S. Lin of Union Chemical Laboratories and Dr. J. R. Pan of Chiao Tung University for their helpful discussions.

Literature Cited

(1) Walling, C. *Acc. Chem. Res.* **1975**, *8*, 125−131.
(2) Ewa, L. K. *Chemosphere* **1991**, *22*, 529−536.
(3) Sedlak, D. L.; Andren, A. W. *Environ. Sci. Technol.* **1991**, *25*, 777−782.
(4) Al-Hayek, N.; Dore, M. N. *Water Res.* **1990**, *24*, 973−982.
(5) Lin, S. S. Ph.D. Dissertation, Drexel University, Philadelphia, PA, 1997.
(6) Valentine, R. L.; Wang, H. C. A. *J. Environ. Eng.* **1998**, *124* (1), 31−38.
(7) Chou, S.; Huang, C. *Chemosphere* **1999**, *38* (12), 2719−2731.
(8) Chou, S.; Huang, C.; Huang, Y. H. *Chemosphere* **1999**, *39* (12), 1997−2006.
(9) Kitajima, N.; Fukuzumi, S. I.; Ono, Y. *J. Phys. Chem.* **1978**, *82*, 1505−1509.
(10) Lin, S. S.; Gurol, M. D. *Environ. Sci. Technol.* **1998**, *32*, 1417−1423.
(11) Levenspiel, O. *Chemical Engineering Reaction*; Wiley-Eastern Limited: New York, 1972.
(12) Chou, S.; Huang, C. *Appl. Catal. A* **1999**, *185*, 237−245.
(13) Buxton, G. V.; Greenstock, C. L.; Helman, W. P.; Ross, A. B. *J. Phys. Chem. Ref. Data* **1988**, *17*, 513−886.
(14) Huang, Y. H.; Huang, G. H.; Chou, S.; You, H. S.; Perng, S. H. Holland patent 1009661, ITRI/Union Chemical Laboratories, 2000.
(15) Sigg, L.; Stumm, W. *Colloids Surf.* **1981**, *2*, 101−117.
(16) Stumm, W. *Chemistry of the Solid−Water Interface*; Wiley-Interscience: New York, 1992.
(17) Calcott, P. H. *Continuous Culture of Cells*, Vol. I; CRC Press: Boca Raton, FL, 1981; p 21.
(18) Kuo, W. G. *Water Res.* **1992**, *26*, 881−886.
(19) Miller, C. M.; Valentine, R. L. *Water Res.* **1995**, *29*, 2353−2359.
(20) Khan, M. A. J.; Watts, R. J. *Water, Air, Soil Pollut.* **1996**, *88*, 247−260.
(21) Stone, A. T. *Environ. Sci. Technol.* **1987**, *21*, 979−988.
(22) Stumm, W.; Sulzberger, B. *Geochim. Cosmochim. Acta* **1992**, *56*, 3233−3257.
(23) McBride, M. B. *Soil Sci. Soc. Am. J.* **1987**, *51*, 1466−1472.
(24) Lu, M. C.; Chen, J. N.; Su, H. S.; Chan, I. C. *Proceedings 22nd Wastewater Treatment Technology Conference*, Taiwan, **1997**; pp 147−154.
(25) Butler, E. C.; Hayes, K. F. *Environ. Sci. Technol.* **1998**, *32*, 1276−1284.

Received for review March 24, 2000. Revised manuscript received November 14, 2000. Accepted November 29, 2000.

ES001129B